

Article

Performance Characteristics and Optimization of a Single-Stage Direct Air Capture Membrane System in Terms of Process Energy Intensity

Kamil Niesporek , Janusz Kotowicz, Oliwia Baszczeńska  and Izabella Maj 

Department of Power Engineering and Turbomachinery, Faculty of Energy and Environmental Engineering, Silesian University of Technology, 44-100 Gliwice, Poland; kamil.niesporek@polsl.pl (K.N.); janusz.kotowicz@polsl.pl (J.K.); oliwia.baszczenska@polsl.pl (O.B.)

* Correspondence: izabella.maj@polsl.pl

Abstract: The increase in emissions and concentration of carbon dioxide in the atmosphere necessitates the implementation of direct carbon dioxide capture technologies. The article presents the characteristics of a single-stage membrane unit for the direct capture of carbon dioxide from the air. A membrane with a selectivity of $\alpha_{\text{CO}_2/\text{N}_2} = 70$ and permeability $P_{\text{CO}_2} = 108 \frac{\text{m}^3(\text{STP})}{(\text{m}^2 \cdot \text{h} \cdot \text{bar})}$ is chosen as the reference variant. It is demonstrated that increasing the pressure difference in the system by reducing the pressure of the permeate stream results in an improvement of all analyzed parameters. Manipulating both the membrane surface and its CO_2 permeability yields similar results. With an increase in permeability or membrane surface area, the proportion of CO_2 in the retentate and permeate decreases, while the degree of carbon dioxide recovery increases. However, the energy intensity of the process is a complex issue due to the presence of a local minimum in the obtained characteristics. Therefore, a relationship between the constants of energy intensity values for the separation process on the surface area field and CO_2 membrane permeability is presented. The minimum energy intensity of the process obtained is 22.5 kWh/kgCO_2 . The CO_2 content in the retentate for all analyses did not exceed 280 ppm.



Citation: Niesporek, K.; Kotowicz, J.; Baszczeńska, O.; Maj, I. Performance Characteristics and Optimization of a Single-Stage Direct Air Capture Membrane System in Terms of Process Energy Intensity. *Energies* **2024**, *17*, 2046. <https://doi.org/10.3390/en17092046>

Academic Editors: Xiaobin Qi and Mingxin Xu

Received: 2 April 2024
Revised: 23 April 2024
Accepted: 24 April 2024
Published: 25 April 2024



Copyright: © 2024 by the authors. Licensee MDPI, Basel, Switzerland. This article is an open access article distributed under the terms and conditions of the Creative Commons Attribution (CC BY) license (<https://creativecommons.org/licenses/by/4.0/>).

Keywords: direct air capture; membrane separation; energy intensity; carbon sequestration; carbon dioxide

1. Introduction

Carbon dioxide is commonly regarded as the leading greenhouse gas (GHG). Despite having a lower global warming potential (GWP) compared to methane or freons, its significant emission from anthropogenic sources and relatively long atmospheric lifespan play a significant role in global warming [1]. The highest emissions of carbon dioxide for years have mainly originated from sectors such as electricity and heat generation and transportation, as well as manufacturing and construction [2]. The mining industry, primarily serving the energy sector, is also characterized by high emissions. Special attention should be paid to coal mines, which, in addition to CO_2 emissions, are responsible for significant amounts of methane emissions [3–5]. The development of renewable energy sources and electrification in sectors like heating or transportation plays a significant role in reducing carbon dioxide emissions. However, the actions taken so far are still insufficient [6]. According to the latest report from the International Energy Agency (IEA) in 2023, there was a 1.1% increase in CO_2 emissions associated with energy alone [7]. Global CO_2 emissions from energy combustion and industrial processes reached 37.2 Gt compared to 36.8 Gt in 2022. Despite a significant increase in the share of renewable energy sources in the global energy structure, emissions are rising, leading to record-high concentrations of carbon dioxide in the atmosphere. As reported by the National Oceanic and Atmospheric Administration (NOAA), which monitors atmospheric conditions, the CO_2 concentration

in May 2022 was 421 ppm compared to about 280 ppm before the industrial era [8]. According to the scenario considering the fulfillment of national commitments to reduce CO₂ emissions by individual countries, the peak of global carbon dioxide emissions from fossil fuel combustion and industrial processes is expected to be achieved before 2030 [9,10]. Continued downward emission trends are projected to lead to significant reductions in CO₂ emissions by 2050, as shown by region in Figure 1 [9]. The Asia–Pacific region has the highest CO₂ emissions, reaching 18,871 Mt CO₂ in 2020. In comparison, the second highest emitting region, North America, reached emissions of 5051 Mt in 2022. By 2050, all regions except Africa are expected to achieve significant emission reductions, with the Asia–Pacific region projected to reduce emissions by about half. However, the scientific community has stressed for years that it may not be possible to meet reduction commitments without the implementation of negative CO₂ emission technologies [11–14]. Consequently, there is a growing focus in the scientific community on the widespread implementation of direct air capture (DAC) technology as a key element towards achieving a net zero emissions (NZE) scenario by 2050 [15,16]. The DAC concept aims to significantly reduce atmospheric CO₂ concentrations in the long term.

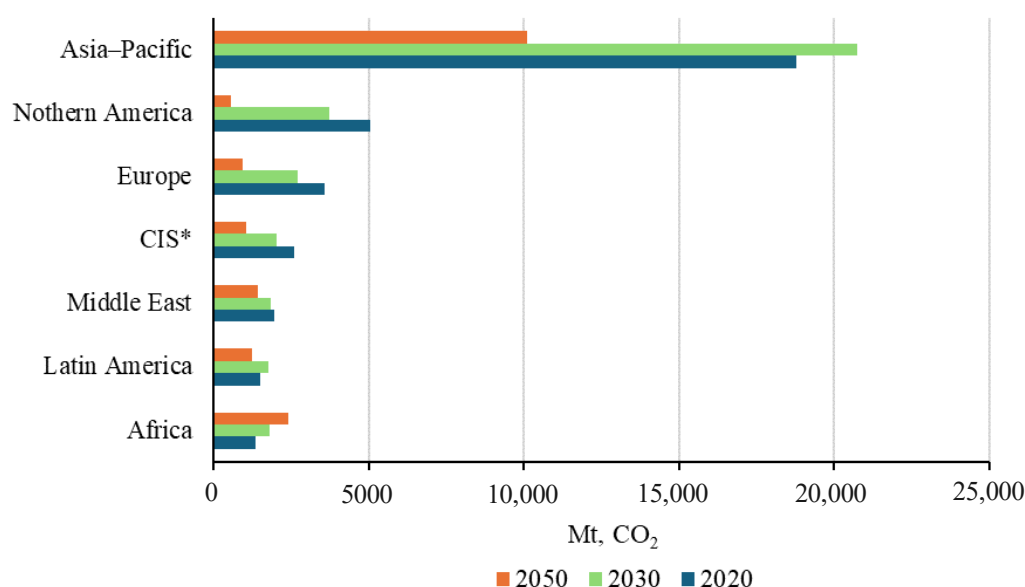


Figure 1. Forecast of CO₂ emissions by region until 2050. * CIS—Commonwealth of Independent States [9].

Unlike traditional carbon dioxide sequestration methods such as carbon capture and storage (CCS) or carbon capture and utilization (CCU), direct air capture relies on the carbon dioxide already present in the atmosphere. Consequently, this process can be conducted independently of emitters [6,17,18]. DAC installations can be located near suitable geological formations for storage or industrial facilities utilizing carbon dioxide as a substrate in various technological processes, such as within Power-to-X technologies [19–23]. This eliminates the need for costly gas transportation over long distances via pipelines. Another advantage of this technology is the potential to reduce carbon dioxide emissions from sources where other methods are not feasible for various reasons. DAC can play a crucial role in reducing carbon dioxide emissions, especially in sectors like aviation, maritime transport, or heavy industry, where electrification is relatively challenging [16–18]. According to the IEA, 27 different DAC installations have been commissioned worldwide so far, with six more under construction [15]. However, there are considerations for at least 130 different projects related to the direct air capture of CO₂. Direct air capture technology has caught the attention of Microsoft, a global leader in the technology industry. Microsoft has committed to achieving negative carbon dioxide emissions by 2030. Part of this goal involves purchasing tokens representing the removal of a certain amount of

carbon dioxide from the atmosphere, which is facilitated by companies specializing in DAC technology [24–26].

While various technologies considered and used in post combustion capture (PCC) can be modified for direct air capture purposes, currently, two technological approaches are employed for capturing CO₂ directly from the atmosphere: liquid (L-DAC) and solid (S-DAC) [15]. In the case of L-DAC, liquid solvents are utilized for carbon dioxide absorption. Although the process is less energy-intensive than S-DAC (approximately 6.5 GJ/t CO₂), sorbent regeneration occurs at high temperatures (300–900 °C) by burning natural gas. S-DAC utilizes porous solid sorbents to capture carbon dioxide on their surface, and due to the lower required operating temperatures (80–120 °C), there is potential to power the process using renewable energy sources. However, the overall energy consumption of the process can reach up to 10 GJ/t CO₂ [15]. The high energy consumption of the process resulting from the low concentration of carbon dioxide in the atmosphere is the main obstacle to the development of DAC technology. The direct air capture of carbon dioxide from the atmosphere consequently entails high costs per ton of captured CO₂. As reported by Kiani et al. [27], the total cost range for L-DAC can vary from 273 to 1227 USD per ton of CO₂ depending on various economic parameters such as electricity, heat price, installation lifespan, and investment costs. However, typically, the estimated cost in the literature ranges from USD 100 to 1000 for both S-DAC and L-DAC, with the prospect of reduction over the years as the still young technology scales up [17,28–32]. Consequently, efforts are underway to develop alternative methods for CO₂ capture from the air.

Membrane separation is a well-established and developed technology proposed as part of the post-combustion capture process [33–39]. Unlike sorption methods, this technology does not require chemicals or an energy-intensive regeneration process. It is characterized by lower investment costs, surface area consumption, and the ease of process operation [40]. Due to its use of only electrical energy, the implementation of direct air capture membrane units may serve as an effective tool for stabilizing the electrical grid in the future, which will be increasingly important with the growing share of renewable energy sources. However, due to the low concentration of carbon dioxide in the atmosphere and the lack of membranes with suitable separation properties, this concept was not considered feasible for DAC for many years. The low permeability of CO₂ membranes requires high pressure differentials in the system or membranes with sufficiently large surface areas for effective gas capture [41]. The required membrane surface area is inversely proportional to the permeability properties [42]. Consequently, this technology seemed unprofitable. However, the situation has changed with the dynamic development of membranes with ultra-high selectivity and permeability for the separated gas, mainly based on polymers [43–45]. For example, Fujikawa et al. announced the development of a membrane with the highest reported CO₂ permeability to date, reaching nearly 40,000 GPU [43]. As a result of membrane advancements in recent years, several publications have emerged regarding the use of membrane technology in DAC installations [40–42,46,47]. However, they are largely review papers on the development of the diaphragm segment in terms of its use in DAC systems. Nevertheless, the concept of a multi-stage membrane DAC unit was discussed in work by Fujikawa et al. [42]. Based on a membrane with a CO₂ permeability of 40,000 GPU and a CO₂/N₂ selectivity of 70, the authors demonstrated the possibility of achieving a 30% carbon dioxide content in the permeate in a four-stage system. They assumed a CO₂ concentration in the retentate of 300 ppm. Additionally, the authors showed that with a membrane permeability of 10,000 GPU and a realistic CO₂/N₂ selectivity of 30, a 40% CO₂ content in the permeate could be achieved. The lack of sufficient research on membrane separation in the context of its use in DAC is noted by Castel et al. [46]. Therefore, the researchers in their work determined the key parameters of a single-stage membrane unit's operation and discussed its capabilities and limitations. They pointed out that in the case of a single-stage membrane separation process based on currently available technologies on the market, the maximum CO₂ content in the permeate could be 2%, and the process

energy consumption is around 18,000 kWh/t CO₂. The energy demand can be minimized through vacuum pumping, but this results in an increase in the membrane surface area.

The literature regarding the characteristics of membrane-based direct air capture systems remains relatively scarce, and the impact of individual process parameters is still relatively poorly understood. This study focused on identifying relationships between changes in selected process parameters and key parameters characterizing membrane separation in a single-stage system. In contrast to existing literature, part of the analysis was conducted in the context of changes in membrane permeability over a wide range, rather than just its selectivity. For membrane DAC technology to effectively compete with sorption methods, it is necessary to understand the relationship between the membrane's sorption capabilities and its surface area in the context of process energy intensity. Therefore, this study paid particular attention to the complexity of carbon dioxide capture energy intensity and proposed an optimization criterion, filling an existing gap in the literature in this area.

2. Materials and Methods

The process of single-stage membrane separation is depicted in the diagram in Figure 2. A unit for the direct capture of carbon dioxide from the air using membrane technology in its simplest single-stage configuration consists of a pre-fan, membrane, and vacuum pump. The pre-fan is responsible for providing slight positive pressure to the atmospheric air to feed the membrane. As a result of membrane separation, the feed stream is separated into the retentate stream and the permeate stream. The retentate stream consists of atmospheric air purified to some extent from carbon dioxide, while the permeate stream contains the separated gas component of certain purity. The efficiency of the membrane separation process is mainly determined by the pressure difference between the feed and permeate [34,35]. To ensure the pressure difference in the system, a vacuum pump is employed.

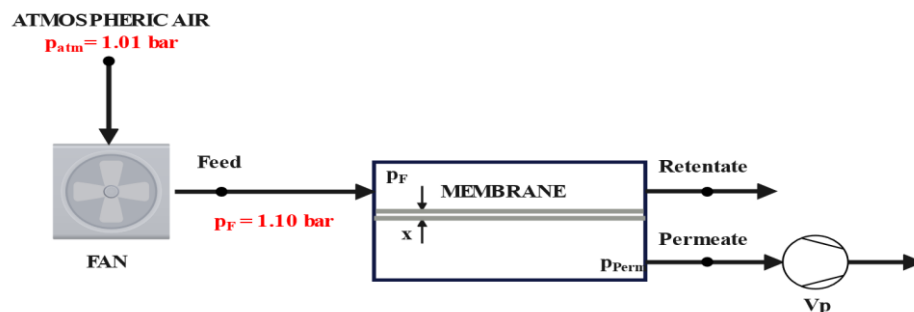


Figure 2. Diagram of a single-stage membrane separation for direct carbon dioxide capture from air. V_p —vacuum pump, p_F —feed pressure, p_{Perm} —permeate pressure, and x —membrane thickness.

To achieve adequate separation process efficiency, membranes must possess high selectivity and permeability for the gas being separated. This is a key area of research in membrane technology development, determining their future applications. In this study, in the initial calculation stage, similar assumptions were adopted as Fujikawa et al. [42]. For calculation purposes, the authors of this study determined the membrane's CO₂ permeability and selectivity based on two different membranes [43,48]. The first consists of free-standing siloxane nanomembrane with a record CO₂ permeability of 40,000 GPU. The second is a multilayer membrane made of Pebax-1657 (Arkema, Colombes, France), with an oxygen plasma-activated poly(dimethylsiloxane) (PDMS) surface used as a gutter layer with a selectivity of 70 CO₂/N₂. Some analyses allow for achieving CO₂ permeability at the level of 50,000 GPU. This is associated with the dynamic development of membrane technology and expected improvements in membrane separation capabilities. Modeling carbon dioxide capture directly from the atmosphere using membrane separation was conducted in Aspen Plus Customer V.12 software, a program that is part of the Aspen Plus V.12 using the Peng-Robinson thermodynamic model. The membrane module consists of

cross-flow capillaries and the separation process is isothermal [34,35]. This software does not allow for the use of permeability expressed in GPU units. Therefore, carbon dioxide permeability expressed in GPU ($1 \text{ GPU} = 7.5 \cdot 10^{-12} \frac{\text{m}^3(\text{STP})}{(\text{m}^2 \cdot \text{s} \cdot \text{Pa})}$) was converted to the units used in the Aspen Plus software, expressed in $\frac{\text{m}^3(\text{STP})}{(\text{m}^2 \cdot \text{h} \cdot \text{bar})}$. The analysis of the simulation results was carried out using Matlab software R2022b. The key calculation assumptions are presented in Table 1. A constant CO₂ fraction in the retentate at the level of 300 ppm, as proposed by Fujikawa et al. [42], was not established. The carbon dioxide fraction in the retentate stream is an outcome and is intended to assess the suitability of membrane technology in DAC systems for reducing atmospheric carbon dioxide concentration and achieving NZE scenarios.

Table 1. Computational assumptions for modelling direct carbon dioxide capture from air in a single-stage membrane separation system.

Parameter	Symbol	Value	Unit
Composition of ambient air:			
-N ₂		78.08	
-O ₂	-	20.95	%
-Ar		0.93	
-CO ₂		0.04	
Molar flux of the feed	n _F	100	kmol/h
Atmospheric pressure	P _{atm}	1.01	bar
Feed pressure	p _F	1.10	bar
Air temperature	T _{Pow}	298.15	K
Isentropic efficiency of pump and fan	η _{is}	90	%
Mechanical efficiency of the pump and fan	η _m	99	%
Membrane selectivity	α _{CO₂/N₂}	70	-
CO ₂ permeability	P _{CO₂}	108	$\frac{\text{m}^3(\text{STP})}{(\text{m}^2 \cdot \text{h} \cdot \text{bar})}$
Membrane surface	A	50	m ²

The parameters, such as the permeation coefficient value P_i (permeability), membrane surface area A, and the partial pressure difference of the separated component across the membrane on both sides, determine the value of the permeate flux [35]. This is described by the following equation:

$$dJ_i = P_i(p_F Z_i - p_{\text{Perm}} Y_i) dA \quad (1)$$

where

Z—the share of the gaseous component in the feed;

Y—the share of the gaseous component in the permeate;

i—gaseous component, e.g., CO₂.

The difference in partial pressures on both sides of the membrane is the driving force behind the separation process. In general, in membrane separation technology, in order to achieve the highest possible pressure difference, treatments such as the following are used [34,35]:

- Increasing the feed pressure;
- Lowering the permeate pressure;
- Increasing the concentration of the permeate component at the membrane inlet;
- Reducing the permeate concentration on the permeate side by using additional sweep gas.

In this study, it was decided to adjust the permeate pressure. A vacuum pump was used to provide the pressure difference between the feed and permeate streams. Therefore, the driving energy of the vacuum pump and the fan supplying air to the membrane is the only energy expenditure. Hence, the energy intensity of the membrane separation process can be determined, for example, in terms of the energy consumed by these flow machines per kilogram of captured CO₂, according to Equation (2). The optimization of the operation of flow machines in terms of power consumption, such as the fan or vacuum pump, is not part of this study. The focus, however, is on parameters directly related to membrane separation, such as permeability, selectivity, membrane surface area, and pressure difference in the system, to understand their overall impact on the energy intensity of the separation process. Therefore, for calculations, a simple single-stage model of the vacuum pump and fan was used, with efficiencies presented in Table 1.

$$E_{\text{sep}} = \frac{N_{\text{elVP}} + N_{\text{elVAN}}}{\dot{m}_{\text{PCO}_2}}, \text{ kWh/kg}_{\text{CO}_2} \quad (2)$$

where

N_{elVP} —the power requirement of the vacuum pump, kW;

N_{elW} —the power requirement of the pre-fan, kW;

\dot{m}_{PCO_2} —CO₂ flow rate in the permeate, kg_{CO₂}/h.

Membrane selectivity is an important parameter that determines the membrane's ability to selectively allow the passage of one or more chemical compounds while blocking the passage of others. It is defined as the ratio of the permeabilities of selected gas components, which for example, for CO₂ and N₂, is presented in Equation (3).

$$\alpha_{\text{CO}_2/\text{N}_2} = \frac{P_{\text{CO}_2}}{P_{\text{N}_2}} \quad (3)$$

According to Table 1, the reference value for membrane selectivity $\alpha_{\text{CO}_2/\text{N}_2}$ is 70, while the permeability of CO₂ is $108 \frac{\text{m}^3(\text{STP})}{(\text{m}^2 \cdot \text{h} \cdot \text{bar})}$. The permeability of other gas components $L(x)$, such as nitrogen, oxygen, and argon, is assumed to be constant relative to each other and depends on the permeability of carbon dioxide P_{CO_2} and the selectivity index $\alpha_{\text{CO}_2/\text{N}_2}$, as described by Equation (4).

$$L(x) = \frac{P_{\text{CO}_2}}{\alpha_{\text{CO}_2/\text{N}_2}} \quad (4)$$

The carbon dioxide recovery rate provides information on the portion of carbon dioxide from atmospheric air that is present in the permeate, as depicted by the following relationship:

$$R = \frac{n_{\text{Perm}}(Y_{\text{CO}_2})}{n_{\text{F}}(Z_{\text{CO}_2})} \quad (5)$$

where

n_{Perm} —permeate molar flux, kmol/h;

n_{F} —permeate molar flux, kmol/h.

3. Results and Discussion

3.1. Effect of Changing Permeate Pressure

In the first stage of calculations, the influence of permeate pressure change on the basic characteristics of the membrane separation unit was determined. Parameters such as the carbon dioxide content in the permeate (Y_{CO_2}) and retentate (X_{CO_2}), recovery rate (R), and energy intensity (E_{sep}) were presented as functions of p_{perm} for the reference membrane with a selectivity of $\alpha_{\text{CO}_2/\text{N}_2} = 70$ and permeability of $P_{\text{CO}_2} = 108 \frac{\text{m}^3(\text{STP})}{(\text{m}^2 \cdot \text{h} \cdot \text{bar})}$.

The membrane surface area was assumed to be $A = 50 \text{ m}^2$ for the calculations. The graphical interpretation of the results for the permeate pressure range of 0.02 bar to 0.1 bar is shown in Figure 3. Changes in pressure were made with a step of 0.01 bar. With an increase in permeate pressure, a decrease in both the recovery rate and the percentage of CO_2 in the permeate can be observed. The greater the pressure difference between the feed stream and the permeate, the more efficient the separation process. By increasing the permeate pressure, we decrease the pressure difference in the system, resulting in a smaller amount of captured CO_2 . Consequently, the carbon dioxide content in the retentate increases. Due to the inefficiency of the process, even with a reduction in the power consumption of the vacuum pump, there is a noticeable increase in energy consumption expressed in kWh per kg of separated CO_2 . Therefore, maximizing the pressure difference is beneficial in terms of achieving the highest recovery rate and CO_2 content in the permeate, and the lowest energy intensity and CO_2 content in the retentate.

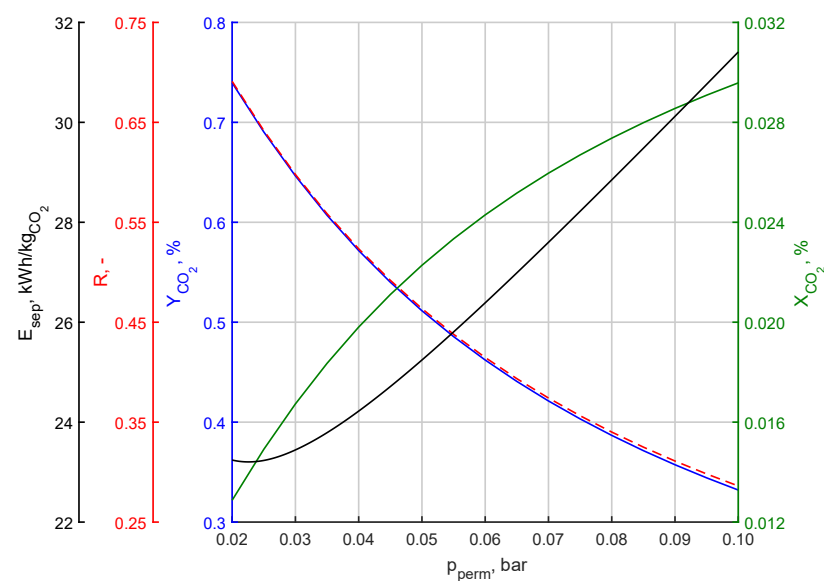


Figure 3. Y_{CO_2} , X_{CO_2} , R , and E_{sep} as a function of permeate pressure.

3.2. Effect of Changing the Membrane Surface

Understanding the impact of pressure changes on key system parameters, the focus was on analyzing the effect of membrane surface area. According to Equation (1), membrane surface area determines the value of the permeating flux through the membrane. It also has economic significance. For the reference membrane, based on the analysis results presented in Figure 2, the lowest permeate pressure was set to $p_{\text{Perm}} = 0.02$ bar. The membrane surfaces were varied in the range from 5 m^2 to 100 m^2 with a step of 5 m^2 . The results are shown in Figure 4. For larger membrane surfaces, the system exhibits a high degree of carbon dioxide recovery. However, the share of CO_2 in the permeate decreases, indicating that the membrane tends to allow other gas components to pass through. Selecting the optimal membrane surface area to minimize the energy intensity of the separation process can be challenging. Both too large and too small membrane surfaces lead to an increase in the energy required to separate 1 kg of carbon dioxide. Therefore, there is an optimum membrane surface area selection to minimize the energy intensity of the carbon dioxide separation process from the air. The minimization of process energy intensity can be observed in the area defined by the intersection points of the characteristics of carbon dioxide content in the permeate and retentate with the recovery degree characteristic. However, an increase in process energy intensity becomes noticeable after exceeding the intersection point of the CO_2 content characteristic in the permeate. If there is a decrease in CO_2 participation in the permeate along with a decrease in its participation in the retentate, it means that the membrane, although capable of separating carbon dioxide, tends to

allow the passage of other gas components. As a result, the gas flow handled by the vacuum pump increases, directly impacting energy intensity in the process. Therefore, the compromise between Y_{CO_2} and the recovery coefficient R , represented by their intersection point on the characteristic as a function of membrane surface area, determines the optimal membrane surface area in terms of energy intensity.

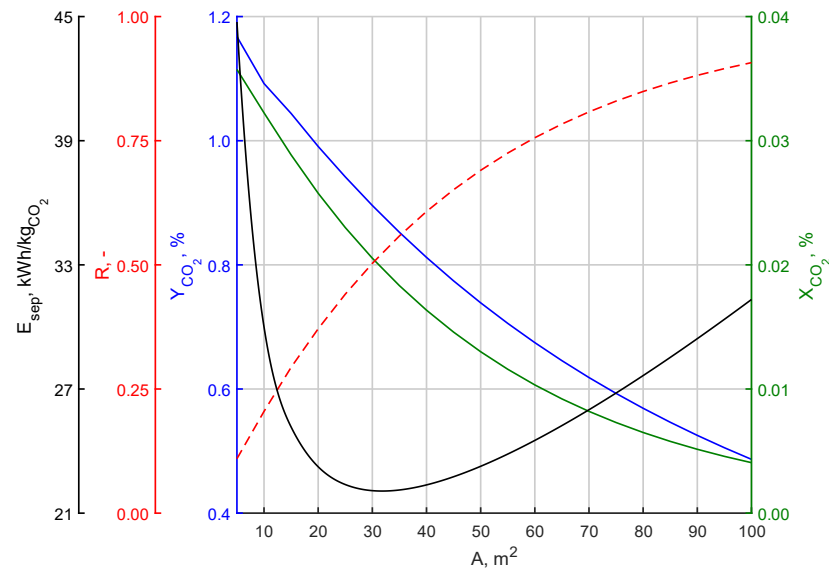


Figure 4. Y_{CO_2} , X_{CO_2} , R , and E_{sep} as a function of membrane surface area for $p_{perm} = 0.02$ bar.

3.3. Effect of Changing the Permeability of Carbon Dioxide

The effect of changing the permeability of CO_2 on the performance characteristics of the membrane separation system was also determined. The analysis was conducted for a membrane selectivity of $\alpha_{CO_2/N_2} = 70$. Again, a permeate pressure of $p_{perm} = 0.02$ bar was applied, and the membrane surface area for calculations was assumed to be $A = 50$ m². The results are presented in Figure 5. Table 2 shows the CO_2 permeability and permeability of other gas components depending on membrane selectivity. The obtained characteristics as a function of changes in permeability are similar in trend to the characteristics obtained as a function of changes in membrane surface area. Both the CO_2 content in the permeate and in the retentate decrease with increasing CO_2 permeability P_{CO_2} across the entire analyzed range. The opposite situation occurs for the purity index of the permeate R . Higher membrane permeability allows for more CO_2 to be recovered in the permeate stream. However, according to the data presented in Table 2, it also affects the increase in the permeability of other gas components, resulting in a decrease in the percentage of CO_2 in the permeate. As a result, a product of low purity is obtained. In the case of energy intensity, a local minimum occurs again. Initially, the energy intensity of the process decreases, but after crossing a certain threshold, it increases with increasing CO_2 permeability. Again, the critical point is the intersection of the characteristics of the CO_2 content of the permeate and the recovery factor. The decrease in the carbon dioxide content of the permeate as the permeability of the membrane increases and its selectivity remains constant can be explained by Equation (4). According to this, as the permeability of CO_2 increases, the permeability of the other gas components also increases, as shown in Table 2. Consequently, the gas flow operated by the vacuum pump increases again, leading to an increased energy intensity of the process.

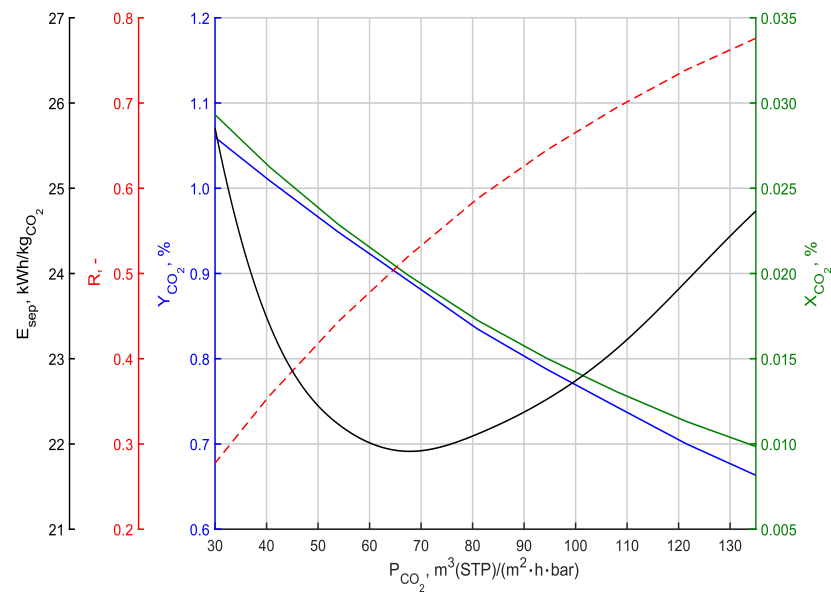


Figure 5. Y_{CO_2} , X_{CO_2} , R , E_{sep} as a function of carbon dioxide permeability P_{CO_2} for permeate pressure $p_{Perm} = 0.02$ bar.

Table 2. The permeability of carbon dioxide and the permeability of other gas components for different values of membrane selectivity.

$P_{CO_2}^*$	P_{CO_2}	$L(x)$		
		α_{CO_2/N_2}		
		70	50	30
GPU	$\frac{m^3(STP)}{(m^2 \cdot h \cdot bar)}$	$\frac{m^3(STP)}{(m^2 \cdot h \cdot bar)}$		
50,000	135.0	1.93	2.70	4.50
45,000	121.5	1.74	2.43	4.05
40,000	108.0	1.54	2.16	3.60
35,000	94.5	1.35	1.89	3.15
30,000	81.0	1.16	1.62	2.70
25,000	67.5	0.96	1.35	2.25
20,000	54.0	0.77	1.08	1.80
15,000	40.5	0.58	0.81	1.35
10,000	27.0	0.39	0.54	0.90

* Carbon dioxide permeability expressed in GPU.

3.4. Effect of Changing Membrane Selectivity

In the next step, the analysis focused on the impact of changing membrane selectivity on the system's performance characteristics. For this purpose, calculations similar to those presented in Figure 5 were repeated for selectivities of $\alpha_{CO_2/N_2} = 50$ and 30. The results are shown in Figure 6. With a change in membrane selectivity, its ability to permeate other gas components also changes, according to Table 2. Comparing Figures 5 and 6, it can be observed that reducing membrane selectivity results in a decrease in the proportion of CO_2 in both the permeate and retentate, while the recovery rate increases. A membrane with higher selectivity thus ensures a better concentration of carbon dioxide in the permeate, but this leads to a greater loss of the separated gas component in the retentate stream. For example, considering a membrane with $\alpha_{CO_2/N_2} = 70$ and a permeability of $P_{CO_2} = 108 \frac{m^3(STP)}{(m^2 \cdot h \cdot bar)}$, the CO_2 content in the permeate is 0.74%. However, for $\alpha = 50$ and 30, it is 0.58% and 0.38%, respectively. Consequently, a multi-stage membrane DAC system based on membranes with lower selectivity will require more separation stages to obtain a permeate with high final purity. Therefore, the use of low-selectivity membranes

is inappropriate, consistent with the results presented in other studies [42,46]. Comparing the recovery rate, it is 69.5% for $\alpha_{\text{CO}_2/\text{N}_2} = 70$, and 76.0% and 83.5% for $\alpha_{\text{CO}_2/\text{N}_2} = 50$ and 30, respectively. With decreasing membrane selectivity, the energy intensity of the process also significantly increases. For example, considering a membrane with a permeability $P_{\text{CO}_2} = 108 \frac{\text{m}^3(\text{STP})}{(\text{m}^2 \cdot \text{h} \cdot \text{bar})}$, the energy intensity of the process was 23.12 kWh/kg_{CO₂}, 27.68 kWh/kg_{CO₂}, and 39.01 kWh/kg_{CO₂} for $\alpha_{\text{CO}_2/\text{N}_2} = 70, 50$, and 30, respectively. In the case of a membrane with $\alpha_{\text{CO}_2/\text{N}_2} = 30$, unlike the other variants, a local minimum occurs for the lowest values of the analyzed carbon dioxide permeabilities.

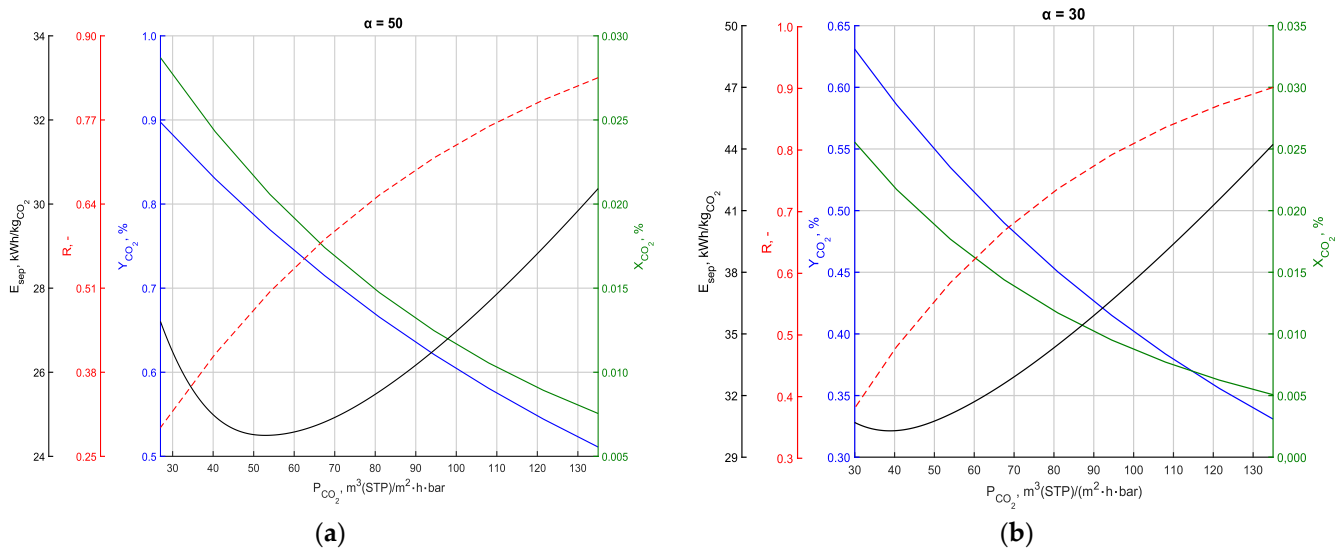


Figure 6. Y_{CO_2} , X_{CO_2} , R , and E_{sep} as a function of carbon dioxide permeability P_{CO_2} for a permeate pressure of $p_p = 0.02$ bar: (a) with membrane selectivity $\alpha_{\text{CO}_2/\text{N}_2} = 50$ and (b) with membrane selectivity $\alpha_{\text{CO}_2/\text{N}_2} = 30$.

3.5. Energy Intensity of the Process

Selecting the appropriate membrane and process parameters is highly challenging. A membrane separation process should be characterized by the highest possible content of the desired gas indicator in the permeate and the highest possible recovery rate. From an energy perspective, the process should also exhibit minimal energy intensity while ensuring the highest possible values of the aforementioned parameters. As mentioned earlier, the driving force of the membrane separation process is the pressure difference across the membrane. Ensuring a greater pressure difference between the feed and the permeate, despite the increased power demand of vacuum pumps, does not necessarily result in increased energy consumption of the process in terms of energy used to separate 1 kg of carbon dioxide, as shown in Figure 3. Properly selected pressure values will affect the efficiency of the separation process by increasing the amount of separated gas component, directly influencing the defined energy intensity expressed in kWh/kg_{CO₂}. To better illustrate the problem, Figure 7a shows the power consumption of flow machines in a single-stage membrane separation process as a function of carbon dioxide permeability for a membrane with parameters $A = 50 \text{ m}^2$ and $\alpha_{\text{CO}_2/\text{N}_2} = 70$. Calculations were performed for various permeate pressures. Figure 7b, on the other hand, shows the energy intensity of the process. The power of the vacuum pump increases with the increasing permeability of CO₂ throughout the analyzed range. This is because, with increasing CO₂ permeability, the permeate flow increases, and thus the flow that the vacuum pump must handle also increases. Due to the constant flow of intake air, the power of the pre-fan remains constant. Comparing both analyses, it is also clear that a greater pressure difference between the feed and the permeate (thus a lower permeate pressure) translates into lower energy intensity of the process of separating 1 kg of carbon dioxide. Only in the case of membranes

with high permeability of the separated gas does the energy intensity of the process for a pressure of 0.02 bar clearly increase, reaching a level corresponding to a pressure of 0.04 bar. Table S1 in the Supplementary Materials contains trend line equations and the coefficient of determination (R^2) for the data presented in Figures 4–7.

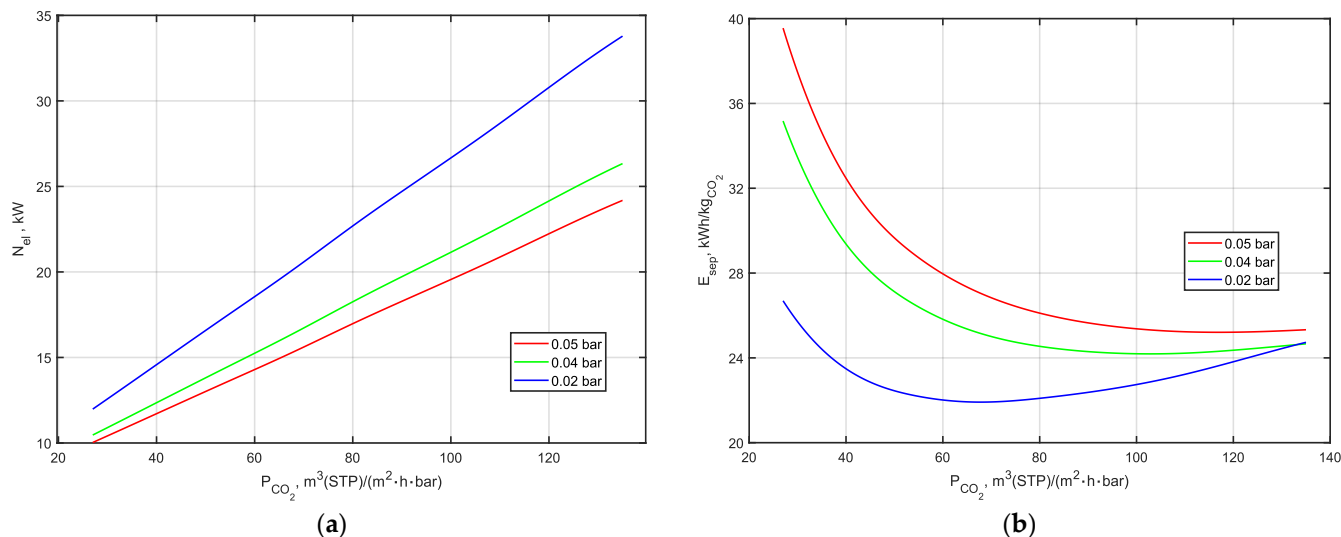


Figure 7. (a) Electrical power demand in a single-stage membrane separation process as a function of CO₂ permeability for various permeate pressure values. (b) Energy intensity of a single-stage membrane separation process as a function of CO₂ permeability for various permeate pressure values.

The above calculations have allowed an understanding of the key dependencies in the single-stage membrane separation system. The problem is to select the appropriate membrane area and permeability to reduce the energy intensity of the process. In order to optimize the system for the energy intensity of capture, the relationship of the constant lines of energy intensity values on the plane of membrane area and permeability will be particularly helpful. These are illustrated in Figure 8a. Additionally, Figure 8b includes similar relationships for power demand. These criteria can be especially useful in modeling multi-stage systems because the first stage of separation significantly influences the outcomes. Due to the highest feed flow rate and low concentration of CO₂ in the first separation stage, it is characterized by the highest electricity demand and energy intensity in kWh/kg_{CO₂}. According to Figure 8a, the lowest energy intensity of the process can be achieved by appropriately selecting the membrane surface area and its CO₂ permeability. The area between the contour lines of 22.5 kWh/kg_{CO₂} corresponds to the minimum energy intensity of the process. According to the contour lines on the graph, for lower values of permeability, to limit the energy intensity of capture, a membrane with a larger surface area should be used. As the permeability of the separated gas increases, the required membrane surface area decreases to minimize the energy intensity of the process. In the case of the electrical power demand of the flow machine, it is lowest for contour lines < 10 kW. Increasing the permeability of the separated gas narrows the range of applicable surface areas for this region.

The results show a similar range of process energy intensity to the work of Fujikawa et al. [42] where membranes with similar permeability and selectivity were analyzed. Additionally, they reveal higher process energy intensity compared to conventionally used sorption methods. As mentioned in the theoretical introduction, the range of energy intensity for conventional methods varies from 6.5 to 10 GJ/kg_{CO₂}, depending on the type of sorbent used [15]. The analyses conducted showed that the lowest energy intensity of the process is 22.5 kWh/kg_{CO₂}. This value corresponds to 81 GJ/kg_{CO₂}. However, a study by Castel et al. [46] showed that the use of ultra-selective experimental membranes can significantly reduce the energy intensity to a level comparable to sorption units. In addition

to the use of membranes with better separation properties, the energy consumption of the process can be reduced by the proper optimization of the flow equipment. As the total compression ratio, the temperature of the compressed gas increases, which directly increases the energy consumption of the vacuum pump and pre-fan. Therefore, the use of intercooling for the vacuum pump can significantly reduce the energy consumption of the process.

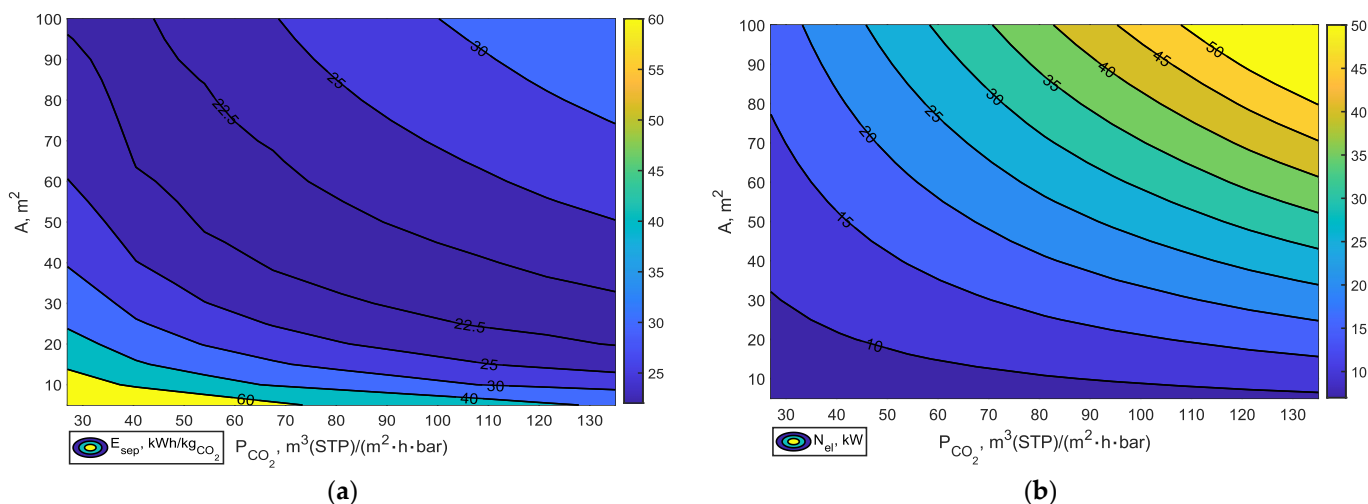


Figure 8. (a) The dependence of the line constants of the values of the energy intensity of the separation process on the plane of the area and CO_2 permeability of the $A - P_{\text{CO}_2}$ membrane. (b) The dependence of the line constants of the value of the consumed electric driving power of the flow machines on the plane of the surface area and CO_2 permeability of the membrane $A - P_{\text{CO}_2}$.

4. Conclusions

The selection of appropriate process parameters and membrane properties for direct carbon capture is highly challenging. This is mainly due to the relatively low concentration of CO_2 in ambient air. Consequently, the membrane should exhibit a high selectivity for the separated gas, as emphasized by various authors and a relationship also demonstrated in this study. For membranes with the highest selectivity, the highest CO_2 content in the permeate and the lowest process energy intensity were achieved. However, a drawback is the reduction in the recovery rate R compared to membranes with lower selectivity. Another crucial aspect is the selection of an appropriate pressure difference between the feed and permeate sides. Increasing this pressure difference by reducing the permeate pressure across the entire range analyzed resulted in improvements in all studied performance characteristics. Even with a significant increase in the electrical power demand of flow machine drive systems, increasing the pressure difference led to a decrease in process energy consumption expressed in $\text{kWh}/\text{kg}_{\text{CO}_2}$. Only for membranes with the highest analyzed permeability did the process energy intensity significantly increase for the highest pressure differences. It was also demonstrated that both changes in membrane surface area and CO_2 permeability shape the system's performance characteristics in a similar manner. With the increase in these parameters, the CO_2 content in both the permeate and retentate decreases, while the recovery rate increases.

Several studies in the literature have highlighted the role of developing high-permeability carbon dioxide membranes to advance the concept of membrane-based direct air capture units. However, from the point of view of the energy intensity of the process, this aspect turns out to be a complex issue due to the presence of a local minimum in the obtained characteristics both as a function of permeability and membrane area. The analyses showed that the increase in CO_2 permeability can contribute to the energy intensity of the process. Therefore, constant lines of process energy intensity values on the membrane surface area and permeability plane were proposed as a convenient tool for optimizing the system's

energy intensity. This is particularly important because, in the case of multi-stage systems, the first separation stage, due to the high feed flow rate with low CO₂ concentration, will largely determine the total process energy intensity. The energy intensity of a membrane plant is high compared to the sorption methods used. However, because there is a gap in the literature regarding the effect of changing individual parameters on the energy intensity of the process, the research presented here focuses on identifying the most important relationships between them, leaving aside the aspect of optimizing the system for the operation of, for example, flow machines. The appropriate optimization of vacuum pump operation by using, for example, inter-cooling can significantly reduce the energy intensity of the process and will be the subject of future studies. In addition, based on the results obtained, future calculations will be based on highly selective membranes to analyze their impact on the energy intensity of the process.

Additionally, the study showed the possibility of achieving a CO₂ content below 280 ppm without CO₂ recovery in the retentate. This could be crucial in efforts to reduce the concentration of CO₂ in ambient air and restore it to pre-industrial levels. A significant portion of the analysis was conducted for membranes with properties reported only experimentally. The implementation of membrane separation within direct air capture processes remains dependent on progress in the field of membranes with high separation capabilities. The identified relationships between the various parameters, especially in the context of process energy intensity, will be used in future studies of multi-stage membrane separation systems. The article did not present an analysis of changes in membrane surface areas for different permeate pressures, which could be the subject of future research. Membranes with larger surface areas can separate a greater amount of the desired gas. However, membranes with larger surface areas also have a greater ability to permeate other gas components, directly influencing the resulting CO₂ content in the permeate, recovery rate, and energy consumption in the process. As demonstrated in the study, the pressure difference between the feed and permeate is one of the key parameters of membrane separation process efficiency. In addition, analyses are planned on the practical feasibility and economic viability of implementing membrane-based direct air capture systems on a larger scale.

Supplementary Materials: The following supporting information can be downloaded at: <https://www.mdpi.com/article/10.3390/en17092046/s1>, Table S1: Trend line equations and coefficient of determination R² for the characteristics shown in Figures 4–7.

Author Contributions: Conceptualization, K.N. and J.K.; methodology, K.N. and J.K.; software, K.N. and O.B.; validation, K.N. and J.K.; formal analysis, K.N.; investigation, K.N.; data curation, K.N. and O.B.; writing—original draft preparation, K.N. and I.M.; writing—review and editing, K.N. and I.M.; visualization, K.N. and O.B.; supervision, J.K.; project administration, J.K.; funding acquisition, I.M. All authors have read and agreed to the published version of the manuscript.

Funding: Research work funded by the statutory research of the Silesian University of Technology.

Data Availability Statement: All data is contained within the article.

Conflicts of Interest: The authors declare no conflicts of interest. The funders had no role in the design of the study; in the collection, analyses, or interpretation of data; in the writing of the manuscript; or in the decision to publish the results.

References

1. The Atmosphere: Getting a Handle on Carbon Dioxide. Available online: <https://science.nasa.gov/earth/climate-change/greenhouse-gases/the-atmosphere-getting-a-handle-on-carbon-dioxide/> (accessed on 26 March 2024).
2. Ritchie, H.; Rosado, P.; Roser, M. Emissions by Sector: Where Do Greenhouse Gases Come From? Available online: <https://ourworldindata.org/emissions-by-sector> (accessed on 21 March 2024).
3. Warmuzinski, K. Harnessing Methane Emissions from Coal Mining. *Process Saf. Environ. Prot.* **2008**, *86*, 315–320. [CrossRef]
4. McKinsey. Climate Risk and Decarbonization: What Every Mining CEO Needs to Know. Available online: <https://www.mckinsey.com/capabilities/sustainability/our-insights/climate-risk-and-decarbonization-what-every-mining-ceo-needs-to-know> (accessed on 23 April 2024).

5. Azadi, M.; Northey, S.A.; Ali, S.H.; Edraki, M. Transparency on Greenhouse Gas Emissions from Mining to Enable Climate Change Mitigation. *Nat. Geosci.* **2020**, *13*, 100–104. [CrossRef]
6. Sanz-Pérez, E.S.; Murdock, C.R.; Didas, S.A.; Jones, C.W. Direct Capture of CO₂ from Ambient Air. *Chem. Rev.* **2016**, *116*, 11840–11876. [CrossRef]
7. IEA. CO₂ Emissions in 2023. 2024. Available online: <https://www.iea.org/reports/co2-emissions-in-2023> (accessed on 21 March 2024).
8. National Oceanic and Atmospheric Administration. Carbon Dioxide Now More than 50% Higher than Pre-Industrial Levels. Available online: <https://www.noaa.gov/news-release/carbon-dioxide-now-more-than-50-higher-than-pre-industrial-levels> (accessed on 24 March 2024).
9. Enerdata. CO₂ Emissions 2050 Forecast: World Trends from Fuel Combustion. Available online: <https://eneroutlook.enerdata.net/forecast-co2-emissions-data-from-fuel-combustion.html> (accessed on 23 April 2024).
10. Duffour, G. Bchin Q Enerdata—Global Energy Trends—2023 Edition. A Troubled, Yet Promising Year for Energy Transition? 2022. Available online: <https://www.enerdata.net/publications/reports-presentations/world-energy-trends.html> (accessed on 1 April 2024).
11. Greig, C.; Uden, S. The Value of CCUS in Transitions to Net-Zero Emissions. *Electr. J.* **2021**, *34*, 107004. [CrossRef]
12. Gasser, T.; Guivarch, C.; Tachiiri, K.; Jones, C.D.; Ciais, P. Negative Emissions Physically Needed to Keep Global Warming below 2 °C. *Nat. Commun.* **2015**, *6*, 7958. [CrossRef]
13. Fuss, S.; Canadell, J.G.; Peters, G.P.; Tavoni, M.; Andrew, R.M.; Ciais, P.; Jackson, R.B.; Jones, C.D.; Kraxner, F.; Nakicenovic, N.; et al. Betting on Negative Emissions. *Nat. Clim. Chang.* **2014**, *4*, 850–853. [CrossRef]
14. Desport, L.; Selosse, S. Perspectives of CO₂ Utilization as a Negative Emission Technology. *Sustain. Energy Technol. Assess.* **2022**, *53*, 102623. [CrossRef]
15. IEA. Direct Air Capture—Energy System. Available online: <https://www.iea.org/energy-system/carbon-capture-utilisation-and-storage/direct-air-capture> (accessed on 25 March 2024).
16. Okonkwo, E.C.; AlNouss, A.; Shahbaz, M.; Al-Ansari, T. Developing Integrated Direct Air Capture and Bioenergy with Carbon Capture and Storage Systems: Progress towards 2 °C and 1.5 °C Climate Goals. *Energy Convers. Manag.* **2023**, *296*, 117687. [CrossRef]
17. IEA. Direct Air Capture. 2022. Available online: <https://www.iea.org/reports/direct-air-capture-2022> (accessed on 25 March 2024).
18. Bouaboula, H.; Chaouki, J.; Belmabkhout, Y.; Zaabout, A. Comparative Review of Direct Air Capture Technologies: From Technical, Commercial, Economic, and Environmental Aspects. *Chem. Eng. J.* **2024**, *484*, 149411. [CrossRef]
19. Quang, D.V.; Milani, D.; Abu Zahra, M. A Review of Potential Routes to Zero and Negative Emission Technologies via the Integration of Renewable Energies with CO₂ Capture Processes. *Int. J. Greenh. Gas Control* **2023**, *124*, 103862. [CrossRef]
20. Mostafa, M.; Antonicelli, C.; Varela, C.; Barletta, D.; Zondervan, E. Capturing CO₂ from the Atmosphere: Design and Analysis of a Large-Scale DAC Facility. *Carbon Capture Sci. Technol.* **2022**, *4*, 100060. [CrossRef]
21. Drechsler, C.; Agar, D.W. Characteristics of DAC Operation within Integrated PtG Concepts. *Int. J. Greenh. Gas Control* **2021**, *105*, 103230. [CrossRef]
22. Daggash, H.A.; Patzschke, C.F.; Heuberger, C.F.; Zhu, L.; Hellgardt, K.; Fennell, P.S.; Bhave, A.N.; Bardow, A.; MacDowell, N. Closing the Carbon Cycle to Maximise Climate Change Mitigation: Power-to-Methanol vs. Power-to-Direct Air Capture. *Sustain. Energy Fuels* **2018**, *2*, 1153–1169. [CrossRef]
23. Motlaghzadeh, K.; Schweizer, V.; Craik, N.; Moreno-Cruz, J. Key Uncertainties behind Global Projections of Direct Air Capture Deployment. *Appl. Energy* **2023**, *348*, 121485. [CrossRef]
24. Joppa, L.; Luers, A.; Willmott, E.; Friedmann, S.J.; Hamburg, S.P.; Broze, R. Microsoft’s Million-Tonne CO₂-Removal Purchase—Lessons for Net Zero. *Nature* **2021**, *597*, 629–632. [CrossRef]
25. The Verge. Microsoft Inks Another Deal to Capture and Store Its Carbon Emissions Underground. Available online: <https://www.theverge.com/2023/3/22/23651587/microsoft-climate-tech-startup-carboncapture-wyoming> (accessed on 25 March 2024).
26. The New York Times. Heirloom Opens First U.S. Direct Air Capture Plant. Available online: <https://www.nytimes.com/2023/11/09/climate/direct-air-capture-carbon.html> (accessed on 25 March 2024).
27. Kiani, A.; Jiang, K.; Feron, P. Techno-Economic Assessment for CO₂ Capture from Air Using a Conventional Liquid-Based Absorption Process. *Front. Energy Res.* **2020**, *8*, 517915. [CrossRef]
28. Fasihi, M.; Efimova, O.; Breyer, C. Techno-Economic Assessment of CO₂ Direct Air Capture Plants. *J. Clean. Prod.* **2019**, *224*, 957–980. [CrossRef]
29. Young, J.; McQueen, N.; Charalambous, C.; Foteinis, S.; Hawrot, O.; Ojeda, M.; Pilorgé, H.; Andresen, J.; Psarras, P.; Renforth, P.; et al. The Cost of Direct Air Capture and Storage Can Be Reduced via Strategic Deployment but Is Unlikely to Fall below Stated Cost Targets. *One Earth* **2023**, *6*, 899–917. [CrossRef]
30. Kulkarni, A.R.; Sholl, D.S. Analysis of Equilibrium-Based TSA Processes for Direct Capture of CO₂ from Air. *Ind. Eng. Chem. Res.* **2012**, *51*, 8631–8645. [CrossRef]
31. Broehm, M.; Strefler, J.; Bauer, N. Techno-Economic Review of Direct Air Capture Systems for Large Scale Mitigation of Atmospheric CO₂. *SSRN Electron. J.* **2015**. [CrossRef]
32. Realmonte, G.; Drouet, L.; Gambhir, A.; Glynn, J.; Hawkes, A.; Köberle, A.C.; Tavoni, M. An Inter-Model Assessment of the Role of Direct Air Capture in Deep Mitigation Pathways. *Nat. Commun.* **2019**, *10*, 3277. [CrossRef]
33. Kárászová, M.; Zach, B.; Petrusová, Z.; Červenka, V.; Bobák, M.; Šyc, M.; Izák, P. Post-Combustion Carbon Capture by Membrane Separation, Review. *Sep. Purif. Technol.* **2020**, *238*, 116448. [CrossRef]

34. Kotowicz, J.; Janusz-Szymańska, K.; Wiciak, G. *Technologie Membranowe Wychwytu Dwutlenku Węgla Ze Spalin Dla Nadkrytycznego Bloku Węglowego*; Wydawnictwo Politechniki Śląskiej: Gliwice, Poland, 2015.
35. Kotowicz, J.; Chmielniak, T.; Janusz-Szymańska, K. The Influence of Membrane CO₂ Separation on the Efficiency of a Coal-Fired Power Plant. *Energy* **2010**, *35*, 841–850. [[CrossRef](#)]
36. Wu, H.; Li, Q.; Guo, B.; Sheng, M.; Wang, D.; Mao, S.; Ye, N.; Qiao, Z.; Kang, G.; Cao, Y.; et al. Industrial-Scale Spiral-Wound Facilitated Transport Membrane Modules for Post-Combustion CO₂ Capture: Development, Investigation and Optimization. *J. Membr. Sci.* **2023**, *670*, 121368. [[CrossRef](#)]
37. Gkotsis, P.; Peleka, E.; Zouboulis, A. Membrane-Based Technologies for Post-Combustion CO₂ Capture from Flue Gases: Recent Progress in Commonly Employed Membrane Materials. *Membranes* **2023**, *13*, 898. [[CrossRef](#)]
38. Carapellucci, R.; Giordano, L.; Vaccarelli, M. Study of a Natural Gas Combined Cycle with Multi-Stage Membrane Systems for CO₂ Post-Combustion Capture. *Energy Procedia* **2015**, *81*, 412–421. [[CrossRef](#)]
39. Merkel, T.C.; Lin, H.; Wei, X.; Baker, R. Power Plant Post-Combustion Carbon Dioxide Capture: An Opportunity for Membranes. *J. Membr. Sci.* **2010**, *359*, 126–139. [[CrossRef](#)]
40. Castro-Muñoz, R.; Zamidi Ahmad, M.; Malankowska, M.; Coronas, J. A New Relevant Membrane Application: CO₂ Direct Air Capture (DAC). *Chem. Eng. J.* **2022**, *446*, 137047. [[CrossRef](#)]
41. Fujikawa, S.; Selyanchyn, R. Direct Air Capture by Membranes. *MRS Bull.* **2022**, *47*, 416–423. [[CrossRef](#)]
42. Fujikawa, S.; Selyanchyn, R.; Kunitake, T. A New Strategy for Membrane-Based Direct Air Capture. *Polym. J.* **2020**, *53*, 111–119. [[CrossRef](#)]
43. Fujikawa, S.; Ariyoshi, M.; Selyanchyn, R.; Kunitake, T. Ultra-Fast, Selective CO₂ Permeation by Free-Standing Siloxane Nanomembranes. *Chem. Lett.* **2019**, *48*, 1351–1354. [[CrossRef](#)]
44. Yoo, M.J.; Kim, K.H.; Lee, J.H.; Kim, T.W.; Chung, C.W.; Cho, Y.H.; Park, H.B. Ultrathin Gutter Layer for High-Performance Thin-Film Composite Membranes for CO₂ Separation. *J. Membr. Sci.* **2018**, *566*, 336–345. [[CrossRef](#)]
45. Bandehali, S.; Ebadi Amooghin, A.; Sanaeepur, H.; Ahmadi, R.; Fuoco, A.; Jansen, J.C.; Shirazian, S. Polymers of Intrinsic Microporosity and Thermally Rearranged Polymer Membranes for Highly Efficient Gas Separation. *Sep. Purif. Technol.* **2021**, *278*, 119513. [[CrossRef](#)]
46. Castel, C.; Bounaceur, R.; Favre, E. Membrane Processes for Direct Carbon Dioxide Capture from Air: Possibilities and Limitations. *Front. Chem. Eng.* **2021**, *3*, 668867. [[CrossRef](#)]
47. Ignatusha, P.; Lin, H.; Kapuscinsky, N.; Scoles, L.; Ma, W.; Patarachao, B.; Du, N. Membrane Separation Technology in Direct Air Capture. *Membranes* **2024**, *14*, 30. [[CrossRef](#)]
48. Selyanchyn, O.; Selyanchyn, R.; Fujikawa, S. Critical Role of the Molecular Interface in Double-Layered Pebax-1657/PDMS Nanomembranes for Highly Efficient CO₂/N₂ Gas Separation. *ACS Appl. Mater. Interfaces* **2020**, *12*, 33196–33209. [[CrossRef](#)]

Disclaimer/Publisher’s Note: The statements, opinions and data contained in all publications are solely those of the individual author(s) and contributor(s) and not of MDPI and/or the editor(s). MDPI and/or the editor(s) disclaim responsibility for any injury to people or property resulting from any ideas, methods, instructions or products referred to in the content.